

# Differentiation of Glioblastoma from Solitary Brain Metastasis Using Apparent Diffusion Coefficient Values and MR Imaging Characteristics

Tritanon O, MD<sup>1</sup>, Chakkaphak K, MD<sup>1</sup>, Jindahra P, MD, PhD, MRCP<sup>2</sup>, Panyaping T, MD<sup>1</sup>

<sup>1</sup> Division of Diagnostic Neuroradiology, Department of Diagnostic and Therapeutic Radiology, Faculty of Medicine, Ramathibodi Hospital, Mahidol University, Bangkok, Thailand

<sup>2</sup> Division of Neurology, Department of Medicine, Faculty of Medicine, Ramathibodi Hospital, Mahidol University, Bangkok, Thailand

**Objective:** To evaluate minimum intratumoral apparent diffusion coefficient (ADC) values, peritumoral ADC values, and magnetic resonance imaging (MRI) characteristics in the differentiation of glioblastoma (GBM) from solitary brain metastasis.

**Materials and Methods:** A cross-sectional study with retrospective review of MRI comparing minimum intratumoral ADC values, peritumoral ADC values, and pre-operative MRI characteristics of 22 patients with GBM and 19 patients with solitary brain metastasis was performed.

**Results:** The minimum intratumoral ADC values and normalized minimum intratumoral ADC ratio of GBM of  $621.64 \pm 145.68 \times 10^{-6}$  mm<sup>2</sup>/second and  $0.84 \pm 0.19$ , respectively, were significantly lower than the values of solitary brain metastasis of  $725.75 \pm 181.64 \times 10^{-6}$  mm<sup>2</sup>/second and  $0.99 \pm 0.23$ . There was no statistically significant difference of minimum peritumoral ADC values and normalized minimum peritumoral ADC ratios between GBM and solitary brain metastasis. MRI characteristics, such as shape of tumor, presence of susceptibility foci, and restricted diffusion of GBM and solitary brain metastasis were significantly different.

**Conclusion:** The minimum intratumoral ADC value was useful in differentiation between GBM and solitary brain metastasis. The minimum intratumoral ADC value and the normalized minimum intratumoral ADC ratio of GBM were significantly lower than those in solitary brain metastasis. Moreover, some MRI characteristics were in favor of differentiation between these two tumor entities including shape of tumor, presence of susceptibility artifact, and restrict diffusion.

**Keywords:** Glioblastoma, Solitary brain metastasis, Apparent diffusion coefficient value, Intratumoral ADC, Peritumoral ADC

J Med Assoc Thai 2019;102(10):1073-81

Website: <http://www.jmatonline.com>

Received 29 Apr 2019 | Revised 22 Jun 2019 | Accepted 29 Jun 2019

Glioblastoma (also called GBM) and brain metastasis are the most common malignant brain tumors encountered in adult population. GBM is the most common primary central nervous system (CNS) neoplasm, representing 15% to 20% of all CNS tumors<sup>(1)</sup>. It derives from glia cell and contains areas of microvascular proliferation and necrosis that aggressively infiltrates the surrounding tissue<sup>(1,2)</sup>. Brain metastases occur in 15% to 40% of patients with

malignancy, and up to 50% of the brain metastases are solitary lesions. A solitary brain metastasis is common in patients with breast, renal cell, colon, and thyroid cancers<sup>(3,4)</sup>.

Differentiation of GBM and solitary brain metastasis is very important and may contribute to better treatment planning<sup>(5-7)</sup>. However, GBM and solitary brain metastasis have overlapping imaging characteristics on conventional magnetic resonance (MR) imaging, i.e., a ring enhancement on contrast enhanced T1-weighted (T1W) images and peritumoral edema on T2-weighted (T2W) images<sup>(8)</sup>.

Diffusion-weighted imaging (DWI) is an imaging technique that provides information about the mobility of microscopic free water diffusion within brain tissue. The apparent diffusion coefficient (ADC) maps represent average diffusion for each voxel.

## Correspondence to:

Panyaping T.

Division of Diagnostic Neuroradiology, Department of Diagnostic and Therapeutic Radiology, Faculty of Medicine, Ramathibodi Hospital, Mahidol University, 270 Rama VI Road, Thung Phaya Thai, Ratchathewi, Bangkok 10400, Thailand.

Phone: +66-2-2011212, Fax: 02-2011297

Email: [theeraphol1@gmail.com](mailto:theeraphol1@gmail.com)

**How to cite this article:** Tritanon O, Chakkaphak K, Jindahra P, Panyaping T. Differentiation of Glioblastoma from Solitary Brain Metastasis Using Apparent Diffusion Coefficient Values and MR Imaging Characteristics. J Med Assoc Thai 2019;102:1073-81.

The ADC values in tumors are inversely correlated with cellularity, which can help grading glioma and characterize the brain tumors<sup>(9-12)</sup>.

Previous studies showed the utilization of ADC in the differentiation of GBM from solitary brain metastasis. The ADC value measurement was performed not only in the intratumoral area but also in the peritumoral edematous area. The idea of different peritumoral ADC values in both entities is based on an observation that GBM frequently infiltrates the surrounding tissue, whereas the metastasis usually displaces the surrounding tissue rather than infiltrates. However, the previous results from intratumoral and peritumoral ADC measurement, distinguishable GBM from solitary brain metastasis, have been controversial<sup>(13-18)</sup>.

The purpose of the present study was to evaluate the minimum intratumoral ADC values, peritumoral ADC values and MR imaging characteristics in the differentiation of GBM from solitary brain metastasis.

## Materials and Methods

The cross-sectional study was conducted in the department of diagnosis and therapeutic radiology of Ramathibodi Hospital between January 2010 and October 2017. The study was approved by the local ethic committee.

### Patients

Forty-one patients diagnosed with GBM and solitary brain metastasis between January 2010 and October 2017 were reviewed. Of these patients, 22 were diagnosed with GBM and 19 had solitary brain metastasis. All patients had pathology-confirmed GBM or brain metastasis, except for six patients with solitary brain metastasis that had not undergone surgery. However, the patients improved on both clinical parameters and the three to six months follow-up MR imaging after brain metastasis treatment. Clinical information regarding age at diagnosis, gender, underlying diseases, status of treatments, and the histopathological results were collected from the medical records.

### Imaging protocol and data acquisition

The MR images were obtained by using a 1.5T (Signa Twin Speed, GE Healthcare) or 3.0T (Ingenia 3T; Philips Healthcare, Best, the Netherlands) with a standard head coil. The MR imaging protocol included axial T1W, T2W, fluid-attenuated inversion recovery (FLAIR), T1W with gadolinium (T1W+Gd), DWI and susceptibility weighted imaging (SWI).

DWI was performed by using a single-shot spin-echo echo-planar image (SSEPI) with the following parameters; repetition time/echo time (TR/TE)=5,400/100 milliseconds, flip angle=90 degrees, section thickness=4 mm with 4 mm gap intersection, and field of view (FOV)=480×220 mm. Diffusion sensitizing gradients were applied sequentially in the x, y, and z directions with b=0 and 1,000 seconds/mm<sup>2</sup>.

The axial T1W, T2W/FS, SWI and T1W+Gd or T1W/FS+Gd were acquired with the following parameter. Axial T1W images were acquired with TR=200, TE=2.3, FOV=240×240, matrix size=320×256, slice thickness 5 mm, intersection gap 1.5 mm. Axial T2W were performed with TR=4,000, TE=70, FOV=240×240, matrix size=400×312, slice thickness 5 mm, intersection gap 1.5 mm. Axial FLAIR performed with TR=9,000, TE=120, FOV=240×240, matrix size=320×224, slice thickness 5 mm, intersection gap 1.5 mm. SWI were recorded with a 3D-fully flow-compensated gradient-echo sequence with the following parameters: TR/TE=27/20 milliseconds, flip angle=15 degrees, section thickness 1 mm with 0.5 mm gap intersection, FOV=390×180 mm.

### Imaging and post-processing analysis

**ADC value measurement:** The ADC value measurements were performed at the PACS workstation for two times with a 2-month interval between each session by a 7-years of experienced neuroradiologist (Tritanon O), who was blinded to the tumor histology. ADC measurement was measured from regions of interest (ROI) drawn at the intratumoral area and peritumoral edema. Circular regions of interest (ROIs) of 10 to 100 mm<sup>2</sup> were manually positioned on ADC maps. Axial T2W, T1W+Gd, SWI images were used as reference images to guide the ROI placement.

For minimum intratumoral ADC measurement, the intratumoral ROI was placed on ADC map within the area that maximum hypointensity corresponded to the enhancing area on post-contrast T1-weighted images, excluding areas of cyst/cavity formation, hemorrhage and/or necrosis. The minimum intratumoral ADC value was automatically calculated on the PACS workstation, called ADC-t.

For peritumoral ADC measurement, the authors selected the image slice, which has the largest peritumoral hyperintensity area on T2W to draw ROIs on ADC maps. Peritumoral ROIs were placed on ADC maps in the maximum hypointensity area, corresponded to peritumoral hyperintense T2 area, and avoided the enhancing areas in three different

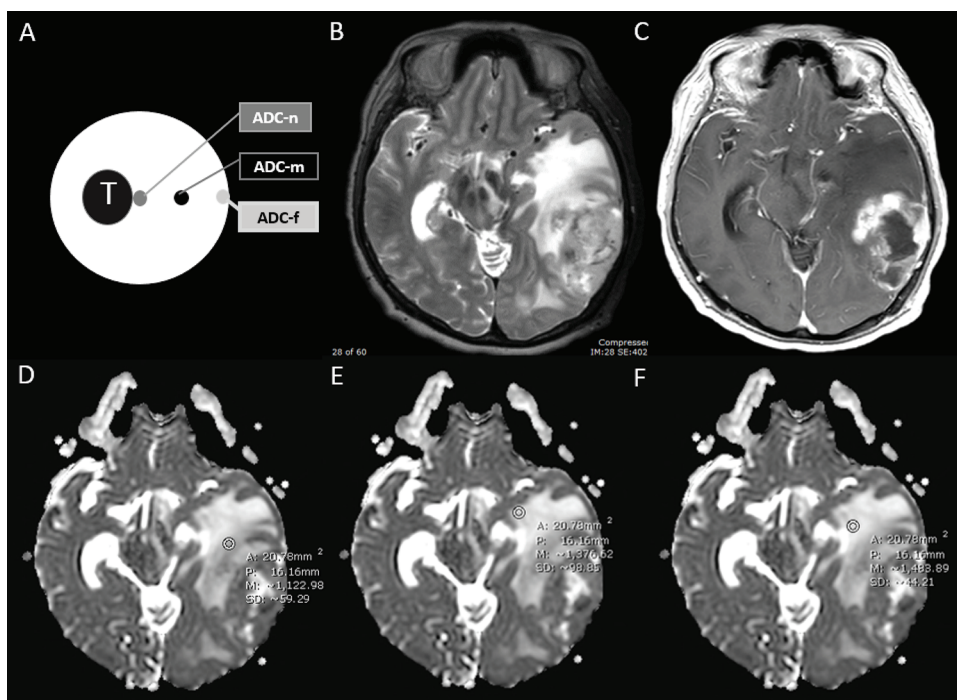


**Figure 1.** The diagram demonstrated measurement of peritumoral ADC values in three different zones of peritumoral edema of the GBM. (A) The diagram demonstrated measurement of peritumoral ADC values in 3 different zones by drawing ROIs in peritumoral edema (white color). (B, C) The GBM (labelled T) showed irregular peripheral enhancing mass (C) with T2 hyperintensity area of peritumoral edema (B). (D-F) On ADC maps, three ROIs were placed in the peritumoral edema corresponding on T2W at (D) the nearest to the enhancing tumor (ADC-n), (E) the farthest from the enhancing tumor (ADC-f) and (F) middle of peritumoral area (ADC-m).

peritumoral zones as following (Figure 1). Zone 1: peritumoral ROI was placed at peritumoral area, which was nearest to the enhancing tumor, called ADC-n. Zone 2: peritumoral ROI was placed at peritumoral area, which was farthest from the enhancing tumor and close to the adjacent normal appearing white matter, called ADC-f. Zone 3: peritumoral ROI was placed in the middle peritumoral edema, called ADC-m. For the controlled ADC value, another ROI was placed in contralateral normal appearing white matter. Finally, the normalized ADC value was calculated as the ratio of the intratumoral ADC value or peritumoral ADC value to the control ADC value.

### MR imaging analysis

The MR imaging findings were independently reviewed at PACS workstation by two neuroradiologists (Tritanon O and Panyaping T) with seven and eight years of experience, respectively. They were blinded to the clinical history and final diagnosis. The MR imaging findings included shape, location of the tumor, cysts or necrosis, presence or absence of susceptibility foci and restricted diffusion, T1W

and T2W signal intensity, and pattern of contrast enhancement. Any discrepancy in the interpretation was resolved by consensus.

### Statistical analysis

Statistical analysis was performed by using statistical software package (Statistical Package for the Social Sciences, version 21; SPSS Inc., Chicago, Illinois). The ADC values were calculated by using intraclass correlation coefficient (ICC). The MR characteristic data were determined by using Cohen K coefficient. Interpretation of the intraclass correlation and Cohen K coefficient were performed according to methods described by Landis and Koch as followed: less than 0, no reproducibility; 0.0 to 0.20, slight reproducibility; 0.21 to 0.40, fair reproducibility; 0.41 to 0.60, moderate reproducibility; 0.61 to 0.80, substantial reproducibility; and 0.81 to 1.00, almost perfect reproducible<sup>(19)</sup>.

Comparisons of continuous variables among the groups were performed by using independent t-test. Chi-square test was used to test categorical variables. A p-value of less than 0.05 was considered a statistical

**Table 1.** The minimum intratumoral ADC value and normalized minimum intratumoral ADC ratio in the GBM and solitary brain metastasis

ADC values and normalized ADC ratio	GBM (n=22) Maen±SD	Metastasis (n=19) Maen±SD	p-value
ADC-t*	621.64±145.68	725.75±181.64	0.049
Normalized ADC-t ratio	0.84±0.19	0.99±0.23	0.033

ADC=apparent diffusion coefficient; GBM=glioblastoma; SD=standard deviation

\* Unit of ADC value:  $\times 10^{-6}$  mm<sup>2</sup>/second

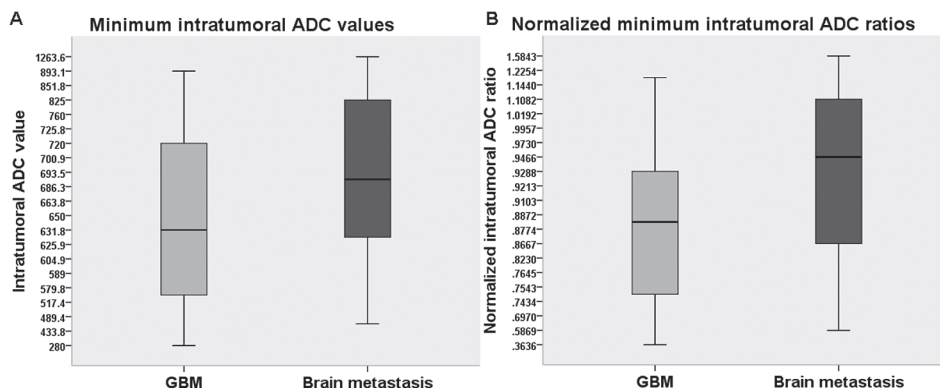


**Figure 2.** (A) Boxplots of minimum intratumoral ADC values ( $\times 10^{-6}$  mm<sup>2</sup>/second). (B) Normalized minimum intratumoral ADC ratios comparing between GBM and solitary brain metastasis.

significant difference.

The ROC curve analysis was performed to determine an optimal cut-off ADC value as well as sensitivity, specificity, positive predictive value (PPV), negative predictive value (NPV), and accuracy in differentiation of GBM from solitary brain metastasis.

## Results

### Patients

Forty-one patients with GBM or solitary brain metastasis were enrolled in the present study. There were 22 patients with GBM (mean age  $\pm$  standard deviation (SD), 54.4 $\pm$ 14.9 years; range 9 to 78 years; 15 men, 7 women) and 19 patients with a solitary brain metastasis (mean age  $\pm$  SD, 57.4 $\pm$ 12.2 years; range 35 to 81 years; 7 men, 12 women). Of the 19 patients with solitary brain metastasis, the primary tumors were eight lung cancers, four breast cancers, two renal cell carcinomas, two cervical cancers, one ovarian cancer, one endometrial cancer, and one gastrointestinal adenocarcinoma.

### ADC values

Intra-rater reliability for ADC value measurements

were ‘substantial to almost perfect’ reproducibility with ICC values of 0.67 to 0.89.

There was statistically significant difference in minimum intratumoral ADC value ( $p=0.049$ ) and normalized minimum intratumoral ADC ratio ( $p=0.03$ ) between GBM and solitary brain metastasis (Table 1). GBM had lower ADC values and lower normalized intratumoral ADC ratio than those in solitary brain metastasis. The box plots of minimum intratumoral ADC values and normalized minimum intratumoral ADC ratios of GBM and solitary brain metastasis are shown in Figure 2.

ROC curve analysis was performed to find out cut-off value in differentiation of GBM from solitary brain metastasis (Figure 3). The cut-off minimum intratumoral ADC value was  $650.4 \times 10^{-6}$  mm<sup>2</sup>/second with 59.1% sensitivity (95% CI 36.4 to 79.3), 68.4% specificity (95% CI 43.5 to 87.4), 68.4% PPV (95% CI 50.6 to 82.1), 59.1% NPV (95% CI 44.5 to 72.2), and 63.4% accuracy (95% CI 46.9 to 77.9). The cut-off normalized minimum intratumoral ADC ratio was 0.921 with 68.2% sensitivity (95% CI 45.1 to 86.1), 63.2% specificity (95% CI 38.4 to 83.7), 68.2% PPV (95% CI 52.7 to 80.5), 63.2% NPV (95% CI 45.9 to 77.6), and 65.9% accuracy (95% CI 49.4 to 79.2).

**Table 2.** The minimum peritumoral ADC values and normalized minimum peritumoral ADC ratios in the GBM and solitary brain metastasis

ADC values and normalized ADC ratios	GBM (n=22) Maen±SD	Metastasis (n=19) Maen±SD	p-value
ADC-n*	1148.38±204.60	1184.05±191.84	0.570
ADC-m+	1403.14±252.70	1409.13±203.10	0.934
ADC-f**	1081.06±198.50	1076.45±179.59	0.939
Normalized ADC-n ratio	1.56±0.28	1.62±0.26	0.507
Normalized ADC-m ratio	1.91±0.37	1.93±0.30	0.860
Normalized ADC-f ratio	1.47±0.28	1.47±0.25	0.992

ADC=apparent diffusion coefficient; GBM=glioblastoma; SD=standard deviation

\* ADC-n: minimum ADC value at peritumoral area which was nearest to the enhancing tumor

\*\* ADC-f: minimum ADC value at peritumoral area which was farthest from the enhancing tumor and close to the adjacent normal appearing white matter

+ ADC-m: minimum ADC measurement at the middle of peritumoral area

\*, \*\*, + Unit of ADC value:  $\times 10^{-6}$  mm<sup>2</sup>/second

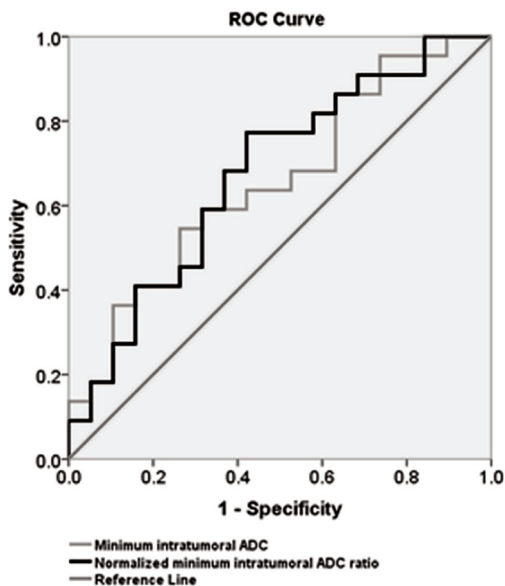


**Figure 3.** ROC curve of the minimum intratumoral ADC value and normalized minimum intratumoral ADC ratio for differentiation of GBM from solitary brain metastasis.

The minimum peritumoral ADC values and normalized minimum peritumoral ADC ratios in the GBM and solitary brain metastasis are presented in Table 2. There was no statistically significant difference of minimum peritumoral ADC values and normalized minimum peritumoral ADC ratios between GBM and solitary brain metastasis.

### MR imaging characteristics

Inter-rater reliability of imaging characteristic determination with Cohen K, showed ‘substantial to almost perfect’ level of reproducibility with K-values of 0.63 to 0.92.

The MR imaging characteristics that were significantly different between GBMs and solitary brain metastasis groups included shape of tumor, presence of restrict diffusion, and susceptibility foci (Table 3). About 95% of GBM appeared as lobulated shape on MR imaging, while solitary brain metastases were demonstrated as lobulated (52.6%), round (42.1%), or oval (5.3%) shapes ( $p=0.03$ ). The presence of restrict diffusion and susceptibility foci were found more commonly in GBM than in solitary brain metastasis ( $p=0.004$ ) (Figure 4).

The MR imaging characteristics, including presence of cystic or necrotic component, T1W and T2W signal intensities, and patterns of enhancement, showed no statistical difference between the two tumor entities.

### Discussion

Many cases of GBM and solitary brain metastasis cannot be differentiated by conventional MR imaging because of their similar imaging features and contrast enhancing patterns<sup>(19,20)</sup>. Differentiation between the two tumor entities has been beneficial for treatment planning and management<sup>(5,6)</sup>.

DWI can assess microscopic water diffusion within the tissue, which has been used as a non-invasive technique for evaluation of the tumor



**Table 3.** Comparison of MR imaging characteristics between GBM and solitary brain metastasis

MR imaging characteristics	GBM (n=22) n (%)	Metastasis (n=19) n (%)	p-value
Maximal tumor diameter (mm), Mean±SD	57.6 ± 16.2	32.5 ± 12.4	0.341
Shape			0.003*
Round	0 (0.0)	8 (42.1)	
Oval	0 (0.0)	1 (5.3)	
Lobulated	21 (95.5)	10 (52.6)	
Irregular	1 (4.5)	0 (0.0)	
Cystic/necrotic component			0.938
Presence	9 (40.9)	8 (42.1)	
Absence	13 (59.1)	11 (57.9)	
Susceptibility foci			0.004*
Presence	22 (100)	13 (68.4)	
Absence	0 (0.0)	6 (31.6)	
Restricted DWI			0.004*
Presence	22 (100)	13 (68.4)	
Absence	0 (0.0)	6 (31.6)	
T1W signal intensity			0.154
Hypointensity	0 (0.0)	1 (5.3)	
Hyperintensity	0 (0.0)	2 (10.5)	
Mixed signal intensity	22 (100)	16 (84.2)	
T2W signal intensity			0.077
Hypointensity	0 (0.0)	1 (5.3)	
Hyperintensity	0 (0.0)	3 (15.8)	
Mixed signal intensity	22 (100)	15 (78.9)	
Pattern of enhancement			0.115
Peripheral/ring enhancement	11 (50.0)	6 (31.6)	
Homogeneous	0 (0.0)	3 (15.8)	
Heterogeneous	11 (50.0)	10 (52.6)	

MR=magnetic resonance; GBM=glioblastoma; SD=standard deviation; DWI=diffusion-weighted imaging; T1W=T1-weighted; T2W=T2-weighted

\* Statistical significant

cellularity. The tumor cellularity is inversely correlated with the tumor ADC values, because the cellular and subcellular elements significantly impede the mobility of water molecules. Thus, the densely cellular regions exhibit lower ADC value<sup>(9)</sup>. The ADC values are used in differentiation of some intracranial tumors<sup>(11)</sup>.

In the present study, the minimum intratumoral ADC and ADC values of different peritumoral areas (ADC-n, ADC-m and ADC-f) were evaluated to distinguish between GBM and solitary brain metastasis. The minimum intratumoral ADC value

and normalized minimum intratumoral ADC ratio in the enhancing area of GBM were lower than those of solitary brain metastasis. The results of the present study were supported by the previous studies from Chiang et al and Mourad et al<sup>(13,17)</sup>. This could be explained by difference in cellularity and histopathological characteristics of the tumors. The GBM has higher cellularity with increased cell membrane destruction and angiogenesis, causing relative decrease in extracellular space and limit water diffusion in the space. Some prior studies also

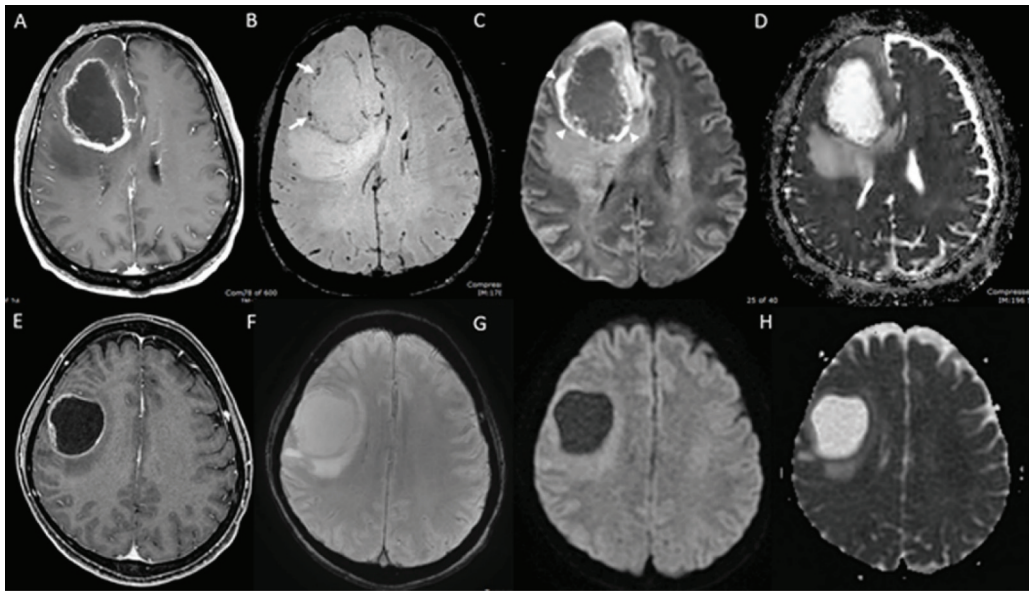


**Figure 4.** (A-D) The top row showed a 57-year-old man with GBM at the right frontal lobe. The GBM appeared as a peripheral enhancing lesion (A) with presence of susceptibility foci (arrow, B) and restricted diffusion (arrow head, C and D). (E-H) The bottom row demonstrated a 57-year-old woman with solitary brain metastasis from breast cancer. There was a peripheral enhancing lesion (E) at the right frontal lobe with absence susceptibility focus (F) or restricted diffusion (G) and (H).

proposed that the ADC value in GBM also reflected the ischemia process and tissue compression effect<sup>(21,22)</sup>. Higher ADC in metastasis was suggested from higher intracellular and extracellular water fraction than GBM<sup>(13,17)</sup>. Moreover, the minimum intratumoral ADC values of GBM and solitary brain metastasis in the present study were lower than the previous studies<sup>(13,17)</sup>. It might be due to different parameters in DWI technique. The authors suggested the optimal minimum intratumoral ADC value of  $650.4 \times 10^{-6}$  mm<sup>2</sup>/second and normalized minimum intratumoral ADC ratio of 0.921, to be used in differentiation of GBM from solitary brain metastasis.

Regarding to the peritumoral ADC value, GBM had infiltrative nature so its peritumoral area represented a combination of vasogenic edema and neoplastic cells infiltration. On the other hands, the peritumoral edema of metastasis was purely vasogenic edema due to the metastatic cells displaced the surrounding tissue<sup>(14)</sup>. However, the present study found no significant difference in minimum peritumoral ADC values and normalized minimum peritumoral ADC ratio between GBM and solitary brain metastasis. The present study also supported the previous reports that the peritumoral ADC values were not useful in differentiating between GBM and solitary brain metastasis<sup>(13,14,18,23)</sup>. This might be

explained by the amount of tumor cell infiltration on the surrounding tissue in GBM was not high enough to lower the ADC values to the level that had significant difference between these two entities. Some studies showed that tumor cell infiltration in surrounding tissue tends to decrease toward the periphery<sup>(6,15)</sup>. In addition, the tumor cell infiltration on the surrounding tissue in GBM was theoretically expected to cause facilitation of water diffusion, resulting in high ADC value<sup>(11,14,24)</sup>. Another possibility may be due to the limitation of small sample size in both groups. Furthermore, some previous studies showed peritumoral ADC value in metastasis was higher than in the GBM, which suggested that the metastasis cause more fluid production than GBM<sup>(17,25,26)</sup>.

Regarding the gender of the patients, 63% of patients with solitary brain metastasis in the present study were women, while 68% of patients with GBMs were men. The difference was explained from the numbers of primary tumors of patients with solitary brain metastasis in the present study, in which 21% of patients had breast cancer and 21% of patients had gynecologic malignancy.

Regarding the imaging characteristics, the present study showed that shapes of the lesion, presence of susceptibility foci, and restricted diffusion could aid in differentiation between GBM and solitary brain

metastasis. The growth pattern and biological nature of GBM affected its shape which generally presented with irregular or lobulated shape. While the solitary brain metastases usually had round shape. Blanchet et al did the semi-automated segmentation and shape description of the tumor, which showed that invasive growth of GBM seems to influence the tumor shape and could be used to differentiate GBM from solitary brain metastasis<sup>(20)</sup>.

All GBM (100%) in the present study had restricted diffusion, while 68.4% of solitary brain metastasis did. This finding was consistent with the aforementioned lower minimum intratumoral ADC values of GBM.

The presence of susceptibility foci reflected blood products or calcifications. These were helpful to distinguish GBM from solitary brain metastasis. The present study found that all GBM (100%) had susceptibility foci, while 68.4% of solitary brain metastasis did. According to GBM is more frequently to have hemorrhage than solitary brain metastasis, although some type of brain metastasis including renal cell carcinoma, lung, and breast cancers also prone to have hemorrhage. The nature of GBM usually has tumor necrosis and hemorrhage. Some previous studies also showed that the higher-grade gliomas had the greater degree of hemorrhage<sup>(27,28)</sup>.

A limitation in the present study was similar to the previous ROI based studies. The subjective manual placement of ROI had affected the accuracy of ADC measurement. In addition, some heterogeneous tumors had cystic or necrotic component and susceptibility foci that causes variation of ADC measurement, especially for the small lesions. However, the authors tried to accurately place the ROIs only in the enhancing solid portion to avoid the susceptibility and necrotic or cystic part to minimize variation.

## Conclusion

The minimum intratumoral ADC value was useful in differentiation between GBM and solitary brain metastasis. The minimum intratumoral ADC value and the normalized minimum intratumoral ADC ratio of GBM were significantly lower than those in solitary brain metastasis. Moreover, some MR imaging characteristics were in favor of differentiation between these two tumor entities including shape of tumor, presence of susceptibility artifact, and restricted diffusion.

## What is already known on this topic?

MR imaging features of glioblastoma and solitary

brain metastasis.

## What this study adds?

- The minimum intratumoral ADC value and the normalized minimum intratumoral ADC ratio of GBM were significantly lower than those in solitary brain metastasis.

- The minimum intratumoral ADC values and normalized minimum intratumoral ADC ratio of GBM of  $621.64 \pm 145.68 \times 10^{-6}$  mm<sup>2</sup>/second and  $0.84 \pm 0.19$ , respectively, were significantly lower than the values of solitary brain metastasis of  $725.75 \pm 181.64 \times 10^{-6}$  mm<sup>2</sup>/second and  $0.99 \pm 0.23$ .

- The cut-off normalized minimum intratumoral ADC ratio was 0.921 with 68.2% sensitivity, 63.2% specificity, 68.2% PPV, 63.2% NPV, and 65.9% accuracy in differentiation of GBM from solitary brain metastasis.

- The cut-off minimum intratumoral ADC value was  $650.4 \times 10^{-6}$  mm<sup>2</sup>/second with 59.1% sensitivity, 68.4% specificity, 68.4% PPV, 59.1% NPV, and 63.4% accuracy in differentiation of GBM from solitary brain metastasis.

- Some MR imaging characteristics are in favor of differentiation between these two tumor entities including shape of tumor, presence of susceptibility artifact, and restricted diffusion

## Acknowledgement

The authors would like to thank Assist. Prof. Sakda Arj-Ong Vallibhakara, MD, PhD, MSIT, MS.IS, BBA, CBA, Department of Clinical Epidemiology and Biostatistics, Ramathibodi Hospital, for assistance with statistical analysis.

## Conflicts of interest

The authors declare no conflict of interest.

## References

1. Kao HW, Chiang SW, Chung HW, Tsai FY, Chen CY. Advanced MR imaging of gliomas: an update. *Biomed Res Int* 2013;2013:970586.
2. Mangiola A, de Bonis P, Maira G, Balducci M, Sica G, Lama G, et al. Invasive tumor cells and prognosis in a selected population of patients with glioblastoma multiforme. *Cancer* 2008;113:841-6.
3. Fink KR, Fink JR. Imaging of brain metastases. *Surg Neurol Int* 2013;4:S209-S219.
4. Barajas RF Jr, Cha S. Imaging diagnosis of brain metastasis. *Prog Neurol Surg* 2012;25:55-73.
5. Campos S, Davey P, Hird A, Pressnail B, Bilbao J, Aviv RI, et al. Brain metastasis from an unknown primary, or primary brain tumour? A diagnostic dilemma. *Curr*



- Oncol 2009;16:62-6.
6. Giese A, Westphal M. Treatment of malignant glioma: a problem beyond the margins of resection. *J Cancer Res Clin Oncol* 2001;127:217-25.
  7. Gately L, McLachlan SA, Dowling A, Philip J. Life beyond a diagnosis of glioblastoma: a systematic review of the literature. *J Cancer Surviv* 2017;11:447-52.
  8. Schwartz KM, Erickson BJ, Lucchinetti C. Pattern of T2 hypointensity associated with ring-enhancing brain lesions can help to differentiate pathology. *Neuroradiology* 2006;48:143-9.
  9. Schaefer PW, Grant PE, Gonzalez RG. Diffusion-weighted MR imaging of the brain. *Radiology* 2000;217:331-45.
  10. Sener RN. Diffusion MRI: apparent diffusion coefficient (ADC) values in the normal brain and a classification of brain disorders based on ADC values. *Comput Med Imaging Graph* 2001;25:299-326.
  11. Yamasaki F, Kurisu K, Satoh K, Arita K, Sugiyama K, Ohtaki M, et al. Apparent diffusion coefficient of human brain tumors at MR imaging. *Radiology* 2005;235:985-91.
  12. Provenzale JM, Mukundan S, Barboriak DP. Diffusion-weighted and perfusion MR imaging for brain tumor characterization and assessment of treatment response. *Radiology* 2006;239:632-49.
  13. Mourad AF, Mohammad HE-dG, Sayed MM, Ragae MA. What's the clinical significance of adding diffusion and perfusion MRI in the differentiation of glioblastoma multiforme and solitary brain metastasis? *Egypt J Radiol Nucl Med* 2017;48:661-9.
  14. Tsougos I, Svolos P, Kousi E, Fountas K, Theodorou K, Fezoulidis I, et al. Differentiation of glioblastoma multiforme from metastatic brain tumor using proton magnetic resonance spectroscopy, diffusion and perfusion metrics at 3 T. *Cancer Imaging* 2012;12:423-36.
  15. Lemercier P, Paz MS, Patrie JT, Flors L, Leiva-Salinas C. Gradient of apparent diffusion coefficient values in peritumoral edema helps in differentiation of glioblastoma from solitary metastatic lesions. *AJR Am J Roentgenol* 2014;203:163-9.
  16. Lee EJ, terBrugge K, Mikulis D, Choi DS, Bae JM, Lee SK, et al. Diagnostic value of peritumoral minimum apparent diffusion coefficient for differentiation of glioblastoma multiforme from solitary metastatic lesions. *AJR Am J Roentgenol* 2011;196:71-6.
  17. Chiang IC, Kuo YT, Lu CY, Yeung KW, Lin WC, Sheu FO, et al. Distinction between high-grade gliomas and solitary metastases using peritumoral 3-T magnetic resonance spectroscopy, diffusion, and perfusion imagings. *Neuroradiology* 2004;46:619-27.
  18. Kono K, Inoue Y, Nakayama K, Shakudo M, Morino M, Ohata K, et al. The role of diffusion-weighted imaging in patients with brain tumors. *AJNR Am J Neuroradiol* 2001;22:1081-8.
  19. Nussbaum ES, Djalilian HR, Cho KH, Hall WA. Brain metastases. Histology, multiplicity, surgery, and survival. *Cancer* 1996;78:1781-8.
  20. Blanchet L, Krooshof PW, Postma GJ, Idema AJ, Goraj B, Heerschap A, et al. Discrimination between metastasis and glioblastoma multiforme based on morphometric analysis of MR images. *AJNR Am J Neuroradiol* 2011;32:67-73.
  21. Higano S, Yun X, Kumabe T, Watanabe M, Mugikura S, Umetsu A, et al. Malignant astrocytic tumors: clinical importance of apparent diffusion coefficient in prediction of grade and prognosis. *Radiology* 2006;241:839-46.
  22. Rose S, Fay M, Thomas P, Bourgeat P, Dowson N, Salvado O, et al. Correlation of MRI-derived apparent diffusion coefficients in newly diagnosed gliomas with [18F]-fluoro-L-dopa PET: what are we really measuring with minimum ADC? *AJNR Am J Neuroradiol* 2013;34:758-64.
  23. Reiche W, Schuchardt V, Hagen T, Il'yasov KA, Billmann P, Weber J. Differential diagnosis of intracranial ring enhancing cystic mass lesions--role of diffusion-weighted imaging (DWI) and diffusion-tensor imaging (DTI). *Clin Neurol Neurosurg* 2010;112:218-25.
  24. Krabbe K, Gideon P, Wagn P, Hansen U, Thomsen C, Madsen F. MR diffusion imaging of human intracranial tumours. *Neuroradiology* 1997;39:483-9.
  25. Lu S, Ahn D, Johnson G, Cha S. Peritumoral diffusion tensor imaging of high-grade gliomas and metastatic brain tumors. *AJNR Am J Neuroradiol* 2003;24:937-41.
  26. Lu S, Ahn D, Johnson G, Law M, Zagzag D, Grossman RI. Diffusion-tensor MR imaging of intracranial neoplasia and associated peritumoral edema: introduction of the tumor infiltration index. *Radiology* 2004;232:221-8.
  27. Ding Y, Xing Z, Liu B, Lin X, Cao D. Differentiation of primary central nervous system lymphoma from high-grade glioma and brain metastases using susceptibility-weighted imaging. *Brain Behav* 2014;4:841-9.
  28. Scatliff JH, Radcliffe WB, Pittman HH, Park CH. Vascular structure of glioblastomas. *Am J Roentgenol Radium Ther Nucl Med* 1969;105:795-805.